Bioorganic Chemistry 37 (2009) 57–63

Contents lists available at ScienceDirect

Bioorganic Chemistry

journal homepage: www.elsevier.com/locate/bioorg

Covalent labeling of nuclear vitamin D receptor with affinity labeling reagents containing a cross-linking probe at three different positions of the parent ligand: Structural and biochemical implications

Taner Kaya [b], Narasimha Swamy [a,1], Kelly S. Persons [a], Swapna Ray [a], Scott C. Mohr [b], Rahul Ray [a,*]

[a] Boston University School of Medicine, 85 East Newton Street, Boston, MA 02118, USA
[b] Boston University, Boston, MA 02215, USA

ARTICLE INFO

Article history:
Received 9 December 2008
Available online 14 February 2009

Keywords:
1α,25-Dihydroxyvitamin D_3
Vitamin D receptor
Vitamin D receptor-ligand-binding domain
Affinity labeling derivatives of 1α,25-dihydroxyvitamin D_3
Growth inhibitory property of 1α,25-dihydroxyvitamin D_3 and its affinity labeling derivatives in keratinocytes
Structural elements in vitamin D receptor-ligand-binding domain
Molecular modeling

ABSTRACT

Structure–functional characterization of vitamin D receptor (VDR) requires identification of structurally distinct areas of VDR-ligand-binding domain (VDR-LBD) important for biological properties of 1α,25-dihydroxyvitamin D_3 ($1,25(OH)_2D_3$). We hypothesized that covalent attachment of the ligand into VDR-LBD might alter 'surface structure' of that area influencing biological activity of the ligand. We compared anti-proliferative activity of three affinity alkylating derivatives of $1,25(OH)_2D_3$ containing an alkylating probe at 1,3 and 11 positions. These compounds possessed high-affinity binding for VDR; and affinity labeled VDR-LBD. But, only the analog with probe at 3-position significantly altered growth in keratinocytes, compared with $1,25(OH)_2D_3$. Molecular models of these analogs, docked inside VDR-LBD tentatively identified Ser237 (helix-3: $1,25(OH)_2D_3$-1-BE), Cys288 (β-hairpin region: $1,25(OH)_2D_3$-3-BE,) and Tyr295 (helix-6: $1,25(OH)_2D_3$-11-BE,) as amino acids that are potentially modified by these reagents. Therefore, we conclude that the β-hairpin region (modified by $1,25(OH)_2D_3$-3-BE) is most important for growth inhibition by $1,25(OH)_2D_3$, while helices 3 and 6 are less important for such activity.

1. Introduction

1α,25-Dihydroxyvitamin D_3 ($1,25(OH)_2D_3$), the dihydroxylated metabolite of vitamin D_3 serves multiple functions. Its biological properties include calcium and phosphorus-homeostasis, growth and maturation-control of a broad range of malignant cells, and immune-regulation. As a result the therapeutic potential of $1,25(OH)_2D_3$ in a broad range of diseases, including mineral homeostatic diseases such as renal osteodystrophy, proliferative diseases such as psoriasis and cancer, and immune-deficiency diseases, such as type I diabetes mellitus is well-recognized [1–7]. However, inherent toxicity of the parent hormone (hypercalcemia, hypercalciuria), particularly at pharmacological doses, has largely precluded its general use as a therapeutic agent. This limitation has spawned a strong interest in developing analogs of $1,25(OH)_2D_3$ that retain intact beneficial effects but display reduced toxicity. Several such analogs have shown promise, but have displayed only a moderate effect clinically in non-toxic doses [8–12]. It is amply clear that rational development of such analogs will require proper understanding of their mechanism of action at the molecular level.

According to current dogma, $1,25(OH)_2D_3$ binds to its nuclear receptor, vitamin D receptor (VDR) in target cells with high specificity; allosterically promoting heterodimerization with the retinoid X receptor (RXR), and binding of the VDR–$1,25(OH)_2D_3$–RXR complex to vitamin D response elements (VDREs) in the vitamin D-regulated genes [e.g., osteopontin, osteocalcin, 1α,25-dihydroxyvitamin D_3-24-hydroxylase (CYP-24)] and recruitment of co-activators to initiate transcription and translation [13,14]. In an alternative proposal apo-VDR, bound to co-repressors, remains transcriptionally inactive till $1,25(OH)_2D_3$ binds to initiate the multi-step transcriptional process. The most important among all the steps in this transcriptional process is highly specific interaction between $1,25(OH)_2D_3$ and VDR. Therefore, structure–functional knowledge, from the sides of both VDR and $1,25(OH)_2D_3$ is

Abbreviations: $1,25(OH)_2D_3$, 1α,25-dihydroxyvitamin D_3; VDR, nuclear vitamin D receptor; reVDR, recombinant vitamin D receptor; VDR-LBD, vitamin D receptor-ligand-binding domain; $1,25(OH)_2D_3$-1-BE, 1α,25-dihydroxyvitamin D_3-1α-(2)-bromoacetate; ^{3}H-$125(OH)_2D_3$-1-BE, 1α,25-dihydroxy[26(27)-^{3}H]vitamin D_3-1α-(2)-bromoacetate; $1,25(OH)_2D_3$-3-BE, 1α,25-dihydroxyvitamin D_3-3β-(2)-bromoacetate; ^{14}C-$1,25(OH)_2D_3$-3-BE, 1α,25-dihydroxyvitamin D_3-3β-[1-^{14}C]-(2)-bromoacetate; $1,25(OH)_2D_3$-6-BE, 1α,25-dihydroxyvitamin D_3-6-propoxy-(2)-bromoacetate; $1,25(OH)_2D_3$-11-BE, 1α25-dihydroxyvitamin D_3-11α-hydroxy-(2)-bromoacetate; ^{14}C-$1,25(OH)_2D_3$-11-BE, 1α,25-dihydroxyvitamin D_3-11α-hydroxy-[1-^{14}C]-(2)-bromoacetate.

* Corresponding author.
E-mail address: bapi@bu.edu (R. Ray).

[1] Deceased.

0045-2068/$ - see front matter © 2009 Elsevier Inc. All rights reserved.
doi:10.1016/j.bioorg.2009.01.001

crucial for a complete understanding of the molecular mechanism of this hormone, as well as development of new generations of $1,25(OH)_2D_3$-based drugs for various diseases with high efficacy and low toxicity.

Recently reports describing the X-ray crystal structures of VDR-LBD, bound to its natural ligand ($1,25(OH)_2D_3$) and several $1,25(OH)_2D_3$-analogs have been published [15–18]. These studies have provided structural evidence for the crucial role played by helix 12 (H-12) in the C-terminal region of VDR in co-activator recruitment and ligand-activated transcriptional process [19]. In addition, a recent study has indicated important role played by H-3 in the transcriptional process and ligand-related activities [20]. Beyond this, there is very little information available about possible role of other structurally distinct areas/features in VDR-LBD that may play an important role in the VDR–$1,25(OH)_2D_3$-mediated transcriptional process.

Mutation in a protein introduces structural/conformational perturbation that is sometimes translated into changes in biological properties related to this protein. We hypothesized that structural perturbation could also be brought about by covalently attaching appendages that mimic the actual ligand to specific areas of the VDR-LBD (chemical modification by "mutated" ligand). Such a change might influence the signal transduction process (as reflected in the biological activity of the ligand) by altering the 'surface structure', micro-environment and polarity of that area of the protein, and that may result in differential recruitment of co-activators for transcription. This way we might be able to identify yet unrecognized structural motifs inside VDR-LBD for the control of the transcriptional process.

Affinity labeling is a classical biochemical method to study interaction between a ligand and its receptor [21]. Such an interaction leads to covalent and specific labeling of the ligand-binding domain by a ligand-analog. In recent times this method has been extended to proteomic studies to investigate protein–protein interaction in complex cellular systems as well.

We have previously demonstrated that 1α,25-dihydroxyvitamin D_3-3-bromoacetate ($1,25(OH)_2D_3$-3-BE), an affinity labeling analog of $1,25(OH)_2D_3$ containing a reactive electrophilic group at the 3-position, covalently labels a single cysteine residue (Cys288) in VDR-LBD [22]. We argued that affinity labeling analogs of $1,25(OH)_2D_3$ with reactive affinity probe attached to various parts of the parent molecule could potentially attach $1,25(OH)_2D_3$ to different parts of the VDR-LBD, and cause perturbation maximally localized in that area; and such a process might be reflected in the biological activities of these analogs. Therefore, in the present study we compared the anti-proliferative activity of three affinity labeling analogs of $1,25(OH)_2D_3$ containing affinity probe at the 1, 3 and 11 positions of the parent molecule. Furthermore, we computationally docked these compounds inside the VDR-LBD crystal coordinates to identify areas of the protein that may be specifically labeled by these compounds, and compared cellular activity of each compound with the parent hormone, $1,25(OH)_2D_3$ in normal human keratinocytes. This communication reports results of these studies, and their implications.

2. Methods

2.1. Synthesis

1α,25-Dihydroxyvitamin D_3-1α-(2)-bromoacetate ($1,25(OH)_2D_3$-1-BE) and 1α,25-dihydroxy[26(27)-^{3}H]vitamin D_3-1α-(2)-bromoacetate (^{3}H-$1,25(OH)_2D_3$-1-BE, specific activity 175 Ci/mmol) and 1α,25-dihydroxyvitamin D_3-3β-(2)-bromoacetate ($1,25(OH)_2D_3$-3-BE) and 1α,25-dihydroxyvitamin D_3-3β-[1-^{14}C]-(2)-bromoacetate (^{14}C-$1,25(OH)_2D_3$-3-BE, specific activity 18.65 mCi/mmol) were synthesized by previously published procedures [23]. 1α,25-Dihydroxyvitamin D_3-6-propoxy-(2)-bromoacetate ($1,25(OH)_2D_3$-6-BE) was obtained by a method described earlier by us [24]. 1α,25-Dihydroxyvitamin D_3-11α-hydroxy-(2)-bromoacetate ($1,25(OH)_2D_3$-11-BE) and 1α,25-dihydroxyvitamin D_3-11α-hydroxy-[1-^{14}C]-(2)-bromoacetate (^{14}C-$1,25(OH)_2D_3$-11-BE, specific activity 18.65 mCi/mmol) were synthesized according to our published procedure [25].

2.2. Recombinant VDR

Full-length recombinant VDR was expressed in *E. coli* as a GST-fusion protein, and purified according to Swamy et al. [26].

2.3. Competitive binding assays of $1,25(OH)_2D_3$-1-BE, $1,25(OH)_2D_3$-3-BE, $1,25(OH)_2D_3$-6-BE and $1,25(OH)_2D_3$-11-BE with reVDR

These assays were carried out by a standard procedure. Typically 50 ng of reVDR was incubated with ^{3}H-$1,25(OH)_2D_3$ (4000 cpm, sp. activity 120 Ci/mmol, Amersham) in the presence of increasing concentrations of $1,25(OH)_2D_3$ or analogs (44.7 fmol–2.4 pmol) in VDR assay buffer (50 mM Tris HCl, 150 mM NaCl, 1.5 mM EDTA, 10 mM sodium molybdate, 5 mM DTT and 0.1% Triton X 100, pH 7.4) for 15 h at 4 °C. Rat liver nuclear extract was included in the binding assays to provide the nuclear accessory factor/s [27]. After the incubation Dextran-coated charcoal was added to remove unbound ^{3}H-$1,25(OH)_2D_3$ and the radioactivity in the supernatants, after centrifugation, was determined by liquid scintillation counting. Assays were carried out in triplicate.

2.4. Affinity labeling studies of reVDR with ^{3}H-$1,25(OH)_2D_3$-1-BE, ^{14}C-$1,25(OH)_2D_3$-3-BE and ^{14}C-$1,25(OH)_2D_3$-11-BE

Samples of reVDR (5 μg) were incubated with 2000 cpm (0.07 nmol) of ^{14}C-$1,25(OH)_2D_3$-3-BE or ^{14}C-$1,25(OH)_2D_3$-11-BE or 10,000 cpm of ^{3}H-$1,25(OH)_2D_3$-1-BE (0.06 fmol) in the presence or in the absence of $1,25(OH)_2D_3$ (1 μg, 2.4 nmol) in 50 mM Tris HCl buffer, pH 7.4 containing 5 mM DTT for 2 h at 4 °C, and reaction was terminated by boiling with SDS–PAGE sample buffer for 5 min. The samples were analyzed by SDS–PAGE, followed by radioactive scanning (^{3}H-containing samples) and phosphorimaging (^{14}C-containing samples).

2.5. Cell culture

Briefly, 3T3 cells were plated at 10^4 cells per 35 mm tissue-culture dish, and were irradiated lethally after 2 days with a ^{60}Co source (5000 rads). Keratinocytes were obtained from neonatal foreskin after overnight trypsinization at 4 °C and treatment with 0.2% EDTA. The cells, in serum-free medium, were plated on lethally-irradiated 3T3 cells. Each experiment was performed on primary or secondary kerationocyte cultures obtained from different skin samples. The serum-free medium consisted of MCDB 153 medium (Sigma Chemical Co.) with additives and calcium (0.15 mM). The cells were grown to 50–60% confluence, when medium was removed and replaced with 1 mL of fresh medium containing either ethanol (0.1% v/v) or various doses of $1,25(OH)_2D_3$ or analogs.

2.6. ^{3}H-Thymidine-incorporation assays

Cells, grown to approximately 50% confluence in MCDB medium were incubated at 37 °C with various concentrations (10^{-10} M and 10^{-8} M) of either $1,25(OH)_2D_3$ or an analog (in 1 μL of ethanol per mL of medium) for 24 h. Each experiment was carried out in triplicate. Control experiments were carried out by incubating cells

with ethanol for the same period of time. After the incubation, medium was removed from each plate and was replaced with ^{3}H-thymidine (one μCi, Sigma–Aldrich Chemical Co., St. Louis, MO) in 1 mL of fresh medium. The cells were incubated at 37 °C for 3 h followed by the removal of the medium and washing with salinated phosphate buffer. The cells were cooled on ice, and 1 mL of ice-cold perchloric acid solution (5%) was added to each dish followed by incubation on ice for 15 min. After the incubation, aqueous medium was removed, and the cells were washed with 1 mL of ice-cold perchloric acid solution, and finally replaced with 1 mL of fresh perchloric acid solution. The cells were incubated in a shaking water bath at 70 °C for 15 min. After this period, medium from each dish was removed, mixed with 10 mL of liquid scintillation cocktail, and counted for radioactivity. Results of this experiment are reported as percentage of cpm for ethanol control for each compound and at each dose level. These results (Fig. 4) are representative of same experiments carried out twice. Statistical analysis was done by student's *t* test.

2.7. Modeling studies

The VDR-LBD structure, taken directly from the co-crystallized protein–ligand complex (Protein Data Bank, PDB ID: 1DB1) was prepared by removing any water molecules, adding hydrogen atoms and assigning Kollman partial charges using Autodock tools before performing actual docking with AutoDock3 suite. Dockings were performed using the Lamarcian Genetic Algorithm (LGA) with default GA parameters using $60 \times 60 \times 60$ grid map calculated by Autogrid. During the run the bromoacetate and hydroxyl groups on the ligand structure were flexible whereas rest of the steroid-derived skeleton was kept rigid in the original conformation. Runs (50 GA) were performed on each analog and results were cross-checked with multiple Simulated Annealing (SA) dockings each with 10(100) runs, varying number of cycles, step parameters and temperature factors, both for partially flexible and fully-flexible performed SA dockings were carried out. The cluster conformations with lowest docked energy (defined as intermolecular interaction energy plus torsional free energy) were manually inspected and superimposed. The amino acid residues in VDR-LBD in close proximity of the carbon atom bearing Br (atom) were identified.

3. Results and discussion

Affinity alkylating derivatives of naturally occurring bio-molecules constitute high-affinity substrate/ligand-analogs that can provide valuable information about the three-dimensional geometries of the substrate/ligand-binding pockets of their cognate proteins including identity of key amino acid residues (contact points) and orientation of the substrate/ligand inside the pocket. The affinity labeling process involves interaction between a nucleophilic amino acid residue in the substrate/ligand-binding pocket with an electrophile in the affinity reagent that lies in close enough proximity to form a covalent bond. In summary, the technique of affinity/photoaffinity labeling, coupled with mutational analysis and functional assay provide a dynamic picture of the binding event between a ligand/substrate with its cognate receptor/enzyme [21].

For the past several years our laboratory has focused on the development of affinity and photaffinity labeling derivatives of $1,25(OH)_2D_3$ to probe VDR-LBD and obtain structure–functional information about VDR–$1,25(OH)_2D_3$ interaction [22,28–31]. In this effort we synthesized $1,25(OH)_2D_3$-3-BE, an affinity labeling derivative of $1,25(OH)_2D_3$, and demonstrated that this compound specifically labels a single Cysteine residue (Cys288) in VDR-LBD [22]. Functional importance of this residue was confirmed by mutation and $1,25(OH)_2D_3$-binding analysis. Additionally we identified several other contact points inside VDR-LBD using Cys288 as the 'docking point' for the 3-hydroxyl group in $1,25(OH)_2D_3$ (*vide infra*). One criticism that is usually leveled at the affinity labeling technique is that the alkylation process could be random, i.e. irrelevant amino acid residue/s in- and/or outside the actual ligand-binding/substrate-binding pocket could be alkylated by these analogs. Our experience, however, is quite different; and we observed that $1,25(OH)_2D_3$-3-BE specifically labeled a single cysteine residue (Cys288) out of three (3) inside the ligand-binding pocket of VDR strongly suggesting that VDR has a very tight binding pocket in the vicinity of the A-ring (of $1,25(OH)_2D_3$). Interestingly Cys288 is one of the conserved Cys residues in the VDR-LBD among other steroid hormone receptors; and prior to our report Nakajima et al. demonstrated a crucial role of Cys288 towards ligand binding [32].

In addition to the demonstration of specific labeling (of VDR-LBD) by $1,25(OH)_2D_3$-3-BE, we established that labeling by $1,25(OH)_2D_3$-3-BE is rapid and quantitative, and labeling process leads to relative stabilization of the holo-VDR-osteocalcin vitamin D responsive element (VDRE) complex. In addition, we observed that $1,25(OH)_2D_3$-3-BE has a considerably stronger anti-proliferative activity compared with $1,25(OH)_2D_3$ in human keratinocytes [31]. So, we asked the question of whether or not other affinity labeling derivatives of $1,25(OH)_2D_3$ containing affinity probes attached at different parts of $1,25(OH)_2D_3$, that can potentially cross-link different sites in the VDR-LBD can have differential cellular effects compared with $1,25(OH)_2D_3$.

As a part of an earlier study we synthesized $1,25(OH)_2D_3$-1-BE, $1,25(OH)_2D_3$-6-BE and $1,25(OH)_2D_3$-11-BE (Fig. 1). Competitive radio-ligand binding assays of four affinity analogs with affinity probe at 1, 3, 6 and 11 positions with reVDR demonstrated half-maximal binding concentrations of $1,25(OH)_2D_3$-1-BE, $1,25(OH)_2D_3$-3-BE,$1,25(OH)_2D_3$-11-BE and $1,25(OH)_2D_3$ (control) are 0.52, 0.18, 0.52 and 0.0015 nmol, respectively. By contrast, $1,25(OH)_2D_3$-6-BE showed no specific binding to VDR (Fig. 2). Therefore, we used $1,25(OH)_2D_3$-1-BE, $1,25(OH)_2D_3$-3-BE,$1,25(OH)_2D_3$-11-BE for subsequent experiments.

Incubation of VDR samples with ^{3}H-$1,25(OH)_2D_3$-1-BE, ^{14}C-$1,25(OH)_2D_3$-3-BE and ^{14}C-$1,25(OH)_2D_3$-11-BE shows that all these compounds covalently label the protein (Fig. 3). However, carrying out the incubation with an excess of $1,25(OH)_2D_3$ significantly reduced labeling in each case indicating specific labeling of VDR-LBD by these compounds (Fig. 3). It should be noted although excess of $1,25(OH)_2D_3$ reduced the intensity of labeling in each case, it did not obliterate cross-linking of the compounds to VDR-LBD. A possible explanation would be that if interaction between the affinity reagent and VDR-LBD is rapid and irreversible, as we have observed [31]), covalently labeled VDR should accumulate with time, even when $1,25(OH)_2D_3$-X-BE ($x = 1, 3, 11$) has to compete with $1,25(OH)_2D_3$ to occupy the binding site in VDR-LBD. Furthermore, as seen in Fig. 3, decrease of labeling (decrease in the intensity of the labeled band) in the presence of a constant amount of $1,25(OH)_2D_3$ varies with different affinity reagents indicating various degrees of competition between $1,25(OH)_2D_3$ and its affinity derivatives. Overall, these results indicated that all these analogs specifically and covalently labeled the $1,25(OH)_2D_3$-binding site in the VDR-LBD.

In our next experiment anti-proliferative activities of $1,25(OH)_2D_3$-1-BE, $1,25(OH)_2D_3$-3-BE and $1,25(OH)_2D_3$-11-BE were compared with $1,25(OH)_2D_3$ at two dose levels. Results of these assays demonstrated that 10^{-8} M of $1,25(OH)_2D_3$ exhibits approximately 20% growth inhibition (Fig. 4). At the same dose $1,25(OH)_2D_3$-3-BE inhibits the growth by approximately 45%. At 10^{-10} M dose level $1,25(OH)_2D_3$ practically has no effect on the growth, while an equmolar amount of $1,25(OH)_2D_3$-3-BE inhibits the growth by approximately 25%. Interestingly, at both doses ef-

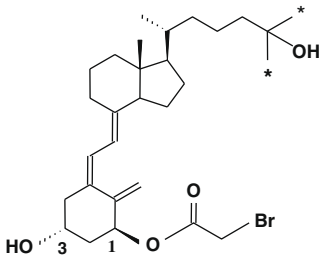

1 α,25-Dihydroxyvitamin D_3-1α-(2)-bromoacetate [**1,25(OH)$_2$D$_3$-1-BE**], and 1α,25-dihydroxy[26(27)-^{3}H] vitamin D_3-1 α-(2)-bromoacetate [**^{3}H-1,25(OH)$_2$D$_3$-1-BE**]

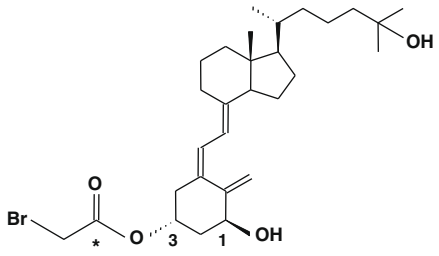

1 α,25-Dihydroxyvitamin D_3-3β-(2)-bromoacetate [**1,25(OH)$_2$D$_3$-3-BE**], and 1α,25-dihydroxyvitamin D_3-3β-[1-^{14}C]-(2)-bromoacetate [**^{14}C-1,25(OH)$_2$D$_3$-3-BE**]

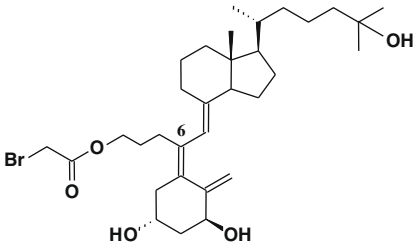

1 α,25-Dihydroxyvitamin D_3-6-propoxy -(2)-bromoacetate [**1,25(OH)$_2$D$_3$-6-BE**]

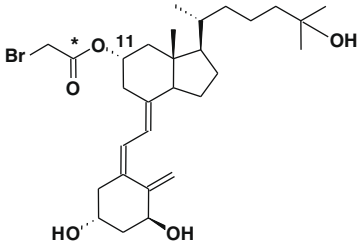

1 α,25-Dihydroxyvitamin D_3-11α-hydroxy -(2)-bromoacetate [**1,25(OH)$_2$D$_3$-11-BE**], and 1 α,25-dihydroxyvitamin D_3-11α-hydroxy-[1-^{14}C] -(2)-bromoacetate [**14C-1,25(OH)$_2$D$_3$-11-BE**],

Fig. 1. Structures of various affinity labeling derivatives of 1,25(OH)$_2$D$_3$ and their radiolabeled counterparts. ∗ Denotes positions of radioisotopes.

fects of 1,25(OH)$_2$D$_3$-1-BE and 1,25(OH)$_2$D$_3$-11-BE are not significantly different from that of 1,25(OH)$_2$D$_3$.

We have demonstrated that 1,25(OH)$_2$D$_3$-1-BE, 1,25(OH)$_2$D$_3$-3-BE and 1,25(OH)$_2$D$_3$-11-BE bind VDR with high and almost equal affinity (Fig. 2), and specifically label VDR-LBD (Fig. 3). Therefore, the growth assay data suggest that simple perturbation of specific areas of VDR-LBD by cross-linking of these analogs might not contribute significantly towards differential growth-inhibitory activity of these compounds in keratinocytes.

Construction of molecular models of these affinity labels, and docking them inside VDR-LBD, based on crystal coordinates identified Ser237, Cys288 and Tyr295 as amino acids that are potentially modified by 1,25(OH)$_2$D$_3$-1-BE, 1,25(OH)$_2$D$_3$-3-BE and 1,25(OH)$_2$D$_3$-11-BE, respectively (Figs. 5–7). Ser237, present in helix-3 has been implicated in ligand-binding by others and us [20,22]. However, according to our growth inhibition assays 1,25(OH)$_2$D$_3$-1-BE is similar to 1,25(OH)$_2$D$_3$ in inhibiting the growth of keratinocytes. A similar conclusion is drawn about helix-6 (containing Tyr295). However, the β-hairpin region, containing Cys288 (contact point

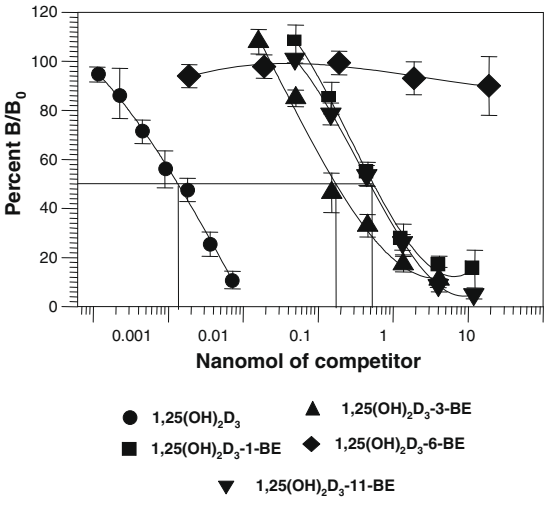

Fig. 2. Competitive radio-ligand binding assay of 1,25(OH)$_2$D$_3$-1-BE, 1,25(OH)$_2$D$_3$-3-BE, 1,25(OH)$_2$D$_3$-6-BE and 1,25(OH)$_2$D$_3$-11-BE with reVDR. Briefly, reVDR was incubated with ^{3}H-1,25(OH)$_2$D$_3$ in the presence of increasing concentrations of 1,25(OH)$_2$D$_3$ or analogs (44.7 fmol–2.4 pmol) for 15 h at 4 °C. After the incubation Dextran-coated charcoal was added to remove unbound ^{3}H-1,25(OH)$_2$D$_3$ and the radioactivity in the supernatants, after centrifugation, was determined by liquid scintillation counting.

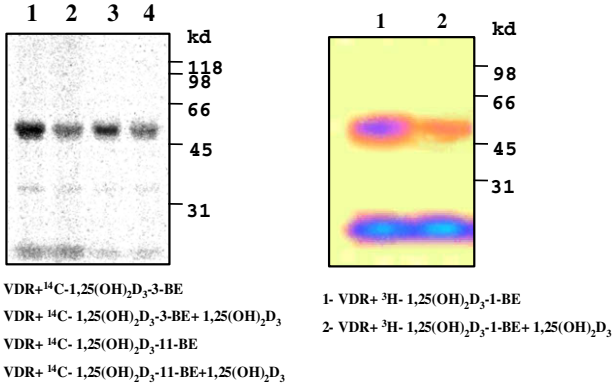

Fig. 3. Affinity labeling of reVDR with ^{3}H-1,25(OH)$_2$D$_3$-1-BE, ^{14}C-1,25(OH)$_2$D$_3$-3-BE and ^{14}C-1,25(OH)$_2$D$_3$-11-BE. Briefly, samples of reVDR were incubated with 2000 cpm (0.07 nmol) of ^{14}C-1,25(OH)$_2$D$_3$-3-BE or ^{14}C-1,25(OH)$_2$D$_3$-11-BE or 10,000 cpm of ^{3}H-1,25(OH)$_2$D$_3$-1-BE (0.06 fmol) in the presence or in the absence of 1,25(OH)$_2$D$_3$ (1 μg, 2.4 nmol) for 2 h at 4 °C, followed by SDS–PAGE analysis and radioactive scanning.

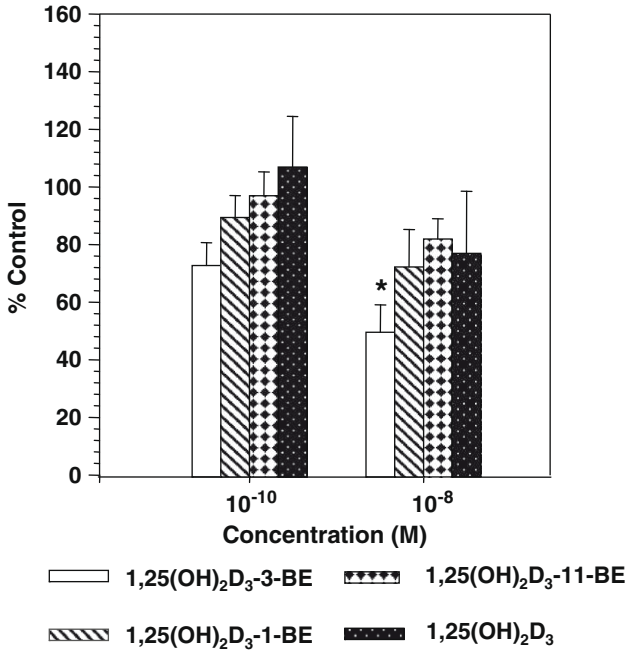

Fig. 4. ^{3}H-thymidine incorporation assay of normal human keratinocytes with $1,25(OH)_2D_3$-1-BE, $1,25(OH)_2D_3$-3-BE, and $1,25(OH)_2D_3$-11-BE. Briefly, keratinocytes were grown to approximately 50% confluence and then incubated with 10^{-10} M or 10^{-8} M of either $1,25(OH)_2D_3$ or an analog for 24 h followed by ^{3}H-thymidine incorporation assay by standard procedure. Each experiment was carried out in triplicate. Control experiments were carried out by incubating cells with ethanol for the same period of time. Results of this experiment are reported as percentage of cpm for ethanol control for each compound and at each dose level. * Represents $p < 0.05$.

for $1,25(OH)_2D_3$-3-BE) is different, and its perturbation lead to modulation of cellular activity. It should be emphasized that Cys288 was implicated to be crucial for ligand-binding in an earlier study by a different group [32]. In addition, in our earlier study we mutated Trp286 and Met284, two neighboring amino acid residues

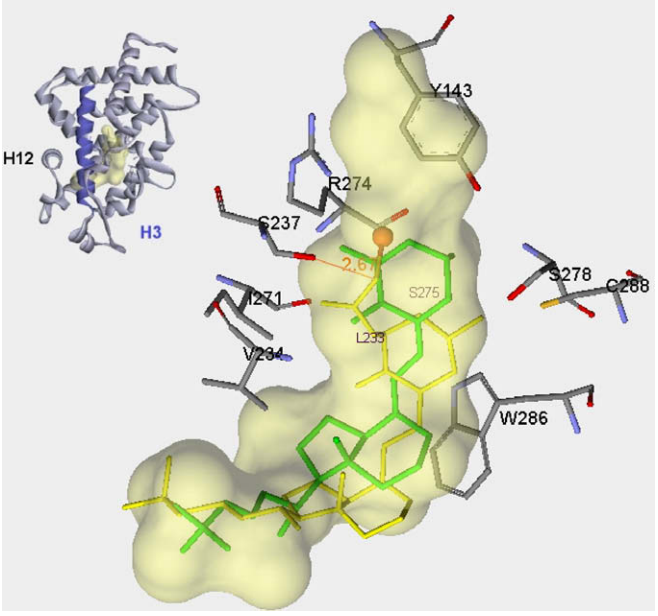

Fig. 5. Molecular modeling of human VDR-LBD with $1,25(OH)_2D_3$-1-BE (green) and $1,25(OH)_2D_3$ (yellow) inside VDR-LBD. Note that the CH2, bearing the Br atom is closest to S237 in helix-3. (For interpretation of the references to color in this figure legend, the reader is referred to the web version of this article.)

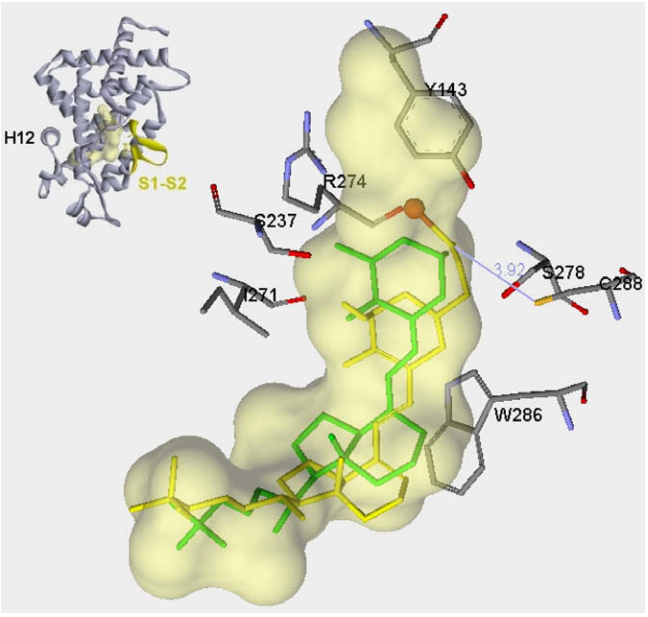

Fig. 6. Molecular modeling of human VDR-LBD with $1,25(OH)_2D_3$-3-BE (green) and $1,25(OH)_2D_3$ (yellow) inside VDR-LBD. Note that the CH2, bearing the Br atom is closest to Cys288 in the base of the β-hairpin loop. (For interpretation of the references to color in this figure legend, the reader is referred to the web version of this article.)

of Cys288 (Fig. 8). Mutation of Trp286 to Ala or Phe almost completely removed $1,25(OH)_2D_3$-binding, while conversion of Met284 to Ser or Ala reduced such binding by approximately 70% [22]. Met284, Trp286 and Cys288 are constituent amino acid residues in the unstructured β-hairpin region. Therefore, we concluded that the β-hairpin region is important for growth-inhibitory prop-

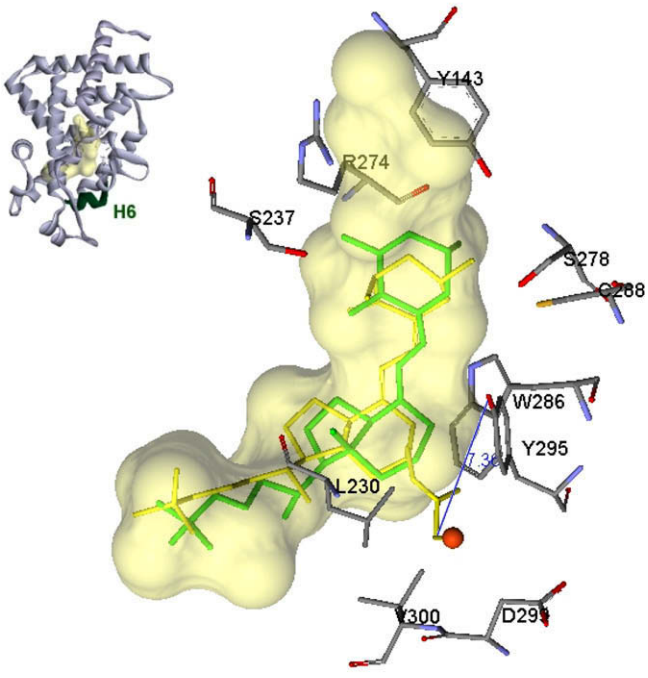

Fig. 7. Molecular modeling of human VDR-LBD with $1,25(OH)_2D_3$-11-BE (green) and $1,25(OH)_2D_3$ (yellow) inside VDR-LBD. Note that the CH2, bearing the Br atom is closest to Tyr295 in helix-6. (For interpretation of the references to color in this figure legend, the reader is referred to the web version of this article.)

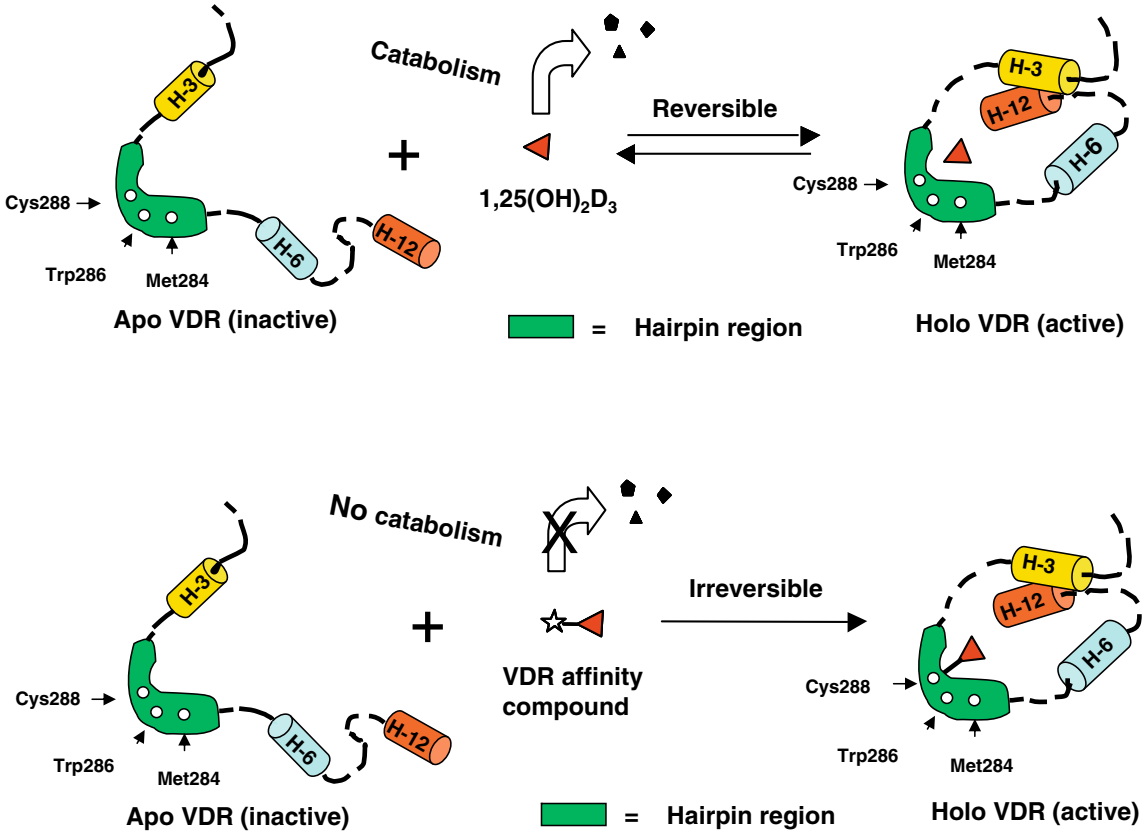

Fig. 8. Cartoon depicting interaction between various amino acid residues inside VDR-LBD with1,25$(OH)_2D_3$ and 1,25$(OH)_2D_3$-affinity analogs. It should be noted that interaction between VDR and 1,25$(OH)_2D_3$ is reversible with possibility of catabolism by the reverse reaction in the steady state. But interaction between VDR-LBD and 1,25$(OH)_2D_3$-affinity labeling analogs is an irreversible process thereby potentially eliminating/reducing catalytic degradation.

erty of 1,25$(OH)_2D_3$, while helices 3 and 6 are less important for such activity.

In recent years our laboratory and others have reported strong agonistic activity of the 3-bromoacetate derivative of 1,25$(OH)_2$-D_3 and 25-hydroxyvitamin D_3, the pre-hormonal precursor of 1,25$(OH)_2D_3$ [33–35]. Previously such activities have been solely attributed to the enhanced catabolic stability of these compounds compared with 1,25$(OH)_2D_3$, as illustrated by the cartoon in Fig. 8. However, our current studies demonstrate that mere catabolic stability of these compounds (by affinity labeling) may not contribute equally towards their cellular activity; and a combination of enhanced catabolic stability and specific area of perturbation (by covalent attachment of the ligand) might be responsible for the enhanced anti-proliferative activity.

In conclusion, majority of structure–function studies have identified helix 12 as the most important structural region of VDR-LBD for the biological activities of 1,25$(OH)_2D_3$ and its analogs. Results of the current study strongly suggest that the β-hairpin region of VDR-LBD might also contribute significantly towards such activities. The 3-bromoacetate derivative of 1,25$(OH)_2D_3$ and 25-hydroxyvitamin D_3 have been projected to have strong potential in several malignancies [33–35]. Therefore, information presented in this communication will be extremely important in providing molecular basis of their action, and develop next generation compounds with enhanced pharmacological properties.

Acknowledgments

This work was supported by grants (to RR) from Department of Defense, Prostate Cancer Research Program (PC 051136), National Cancer Institute of the National Institutes of Health (1R41 CA126317-01A1 and 1R21 CA127629-01A2), and Community Technology Fund, Boston University. The authors would also like to thank Dr. Sandor Vajda, College of Engineering, Boston University.

References

[1] G. Eelen, C. Gysemans, L. Verlinden, E. Vanoirbeek, P. De Clercq, D. Van Haver, C. Mathieu, R. Bouillon, A. Verstuyf, Curr. Med. Chem. 14 (2007) 1893–1910.
[2] R. Bouillon, G. Eelen, L. Verlinden, C. Mathieu, G. Carmeliet, A. Verstuyf, J. Steroid Biochem. Mol. Biol. 102 (2006) 156–162.
[3] S. Matsuda, G. Jones, Mol. Cancer Ther. 5 (2006) 797–808.
[4] X. Palomer, J.M. González-Clemente, F. Blanco-Vaca, D. Mauricio, Diabetes Obes. Metab. 10 (2008) 185–197.
[5] M.J. Campbell, L. Adorini, Expert Opin. Ther. Targets 10 (2006) 735–748.
[6] G. Penna, S. Amuchastegui, G. Laverny, L. Adorini, J. Bone Miner. Res. 22 (Suppl. 2) (2007) V69–V73.
[7] C. Gysemans, E. van Etten, L. Overbergh, A. Giulietti, G. Eelen, M. Waer, A. Verstuyf, R. Bouillon, C. Mathieu, Diabetes 57 (2008) 269–275.
[8] C.S. Johnson, J.R. Muindi, P.A. Hershberger, D.L. Trump, Anticancer Res. 26 (2006) 2543–2549.
[9] D.L. Trump, P.A. Hershberger, R.J. Bernardi, S. Ahmed, J. Muindi, M. Fakih, W.D. Yu, C.S. Johnson, J. Steroid Biochem. Mol. Biol. 89–90 (2004) 519–526.
[10] J.R. Wu-Wong, J. Tian, D. Goltzman, Curr. Opin. Invest. Drugs 5 (2004) 320–326.
[11] K. Dalhoff, J. Dancey, L. Astrup, T. Skovsgaard, K.J. Hamberg, F.J. Lofts, O. Rosmorduc, S. Erlinger, J. Bach Hansen, W.P. Steward, T. Skov, F. Burcharth, T.T. Evans, Brit. J. Cancer 89 (2003) 252–257.
[12] T.R. Evans, K.W. Colston, F.J. Lofts, D. Cunningham, D.A. Anthoney, H. Gogas, J.S. de Bono, K.J. Hamberg, T. Skov, J.L. Mansi, Brit. J. Cancer 86 (2002) 680–685.
[13] M.B. Demay, Ann. NY Acad. Sci. 1068 (2006) 204–213.
[14] A.L. Sutton, P.N. MacDonald, Mol. Endocrinol. 17 (2003) 777–791.
[15] N. Rochel, J.M. Wurtz, A. Mitschler, B. Klaholz, D. Moras, Mol. Cell 5 (2000) 173–179.
[16] N. Rochel, S. Hourai, X. Pérez-García, A. Rumbo, A. Mourino, D. Moras, Arch. Biochem. Biophys. 460 (2007) 172–176.
[17] G. Tocchini-Valentini, N. Rochel, J.M. Wurtz, D. Moras, J. Med. Chem. 47 (2004) 1956–1961.

[18] J.L. Vanhooke, B.P. Tadi, M.M. Benning, L.a. Plum, H.F. DeLuca, Arch. Biochem. Biophys. 460 (2007) 161–165.
[19] S. Väisänen, M. Peräkylä, J.I. Kärkkäinen, A. Steinmeyer, C. Carlberg, J. Mol. Biol. 315 (2002) 229–238.
[20] A.M. Jiménez-Lara, A. Aranda, J. Biol. Chem. 274 (1999) 13503–13510.
[21] F.W. Sweet, G.L. Murdock, Endocr. Rev. 8 (1987) 154–184.
[22] N. Swamy, W. Xu, N. Paz, J.C. Hsieh, M.R. Haussler, G.J. Maalouf, S.C. Mohr, R. Ray, Biochemistry 39 (2000) 12162–12171.
[23] R. Ray, N. Swamy, P.N. MacDonald, S. Ray, M.R. Haussler, M.F. Holick, J. Biol. Chem. 271 (1996) 2012–2017.
[24] J.K. Addo, N. Swamy, R. Ray, Steroids 64 (1999) 273–282.
[25] N. Swamy, J.K. Addo, M.R. Vskokovic, R. Ray, Arch. Biochem. Biophys. 373 (2000) 471–478.
[26] N. Swamy, S.C. Mohr, W. Xu, R. Ray, Arch. Biochem. Biophys. 363 (1999) 219–226.
[27] S. Nakajima, J.C. Hsieh, P.N. MacDonald, C.A. Haussler, M.A. Galligan, P.W. Jurutka, M.R. Haussler, Biochem. Biophys. Res. Commun. 197 (1993) 478–485.
[28] R. Ray, S. Rose, S.A. Holick, M.F. Holick, Biochem. Biophys. Res. Commun. 132 (1985) 198–203.
[29] R. Ray, M.F. Holick, Steroids 51 (1988) 623–630.
[30] R. Ray, S. Ray, S. Rose, M.F. Holick, Steroids 58 (1993) 462–465.
[31] M.L. Chen, S. Ray, N. Swamy, M.F. Holick, R. Ray, Arch. Biochem. Biophys. 370 (1999) 34–44.
[32] S. Nakajima, J.C. Hsieh, P.W. Jurutka, M.A. Galligan, C.A. Haussler, G.K. Whitfield, M.R. Haussler, J. Biol. Chem. 271 (1996) 5143–5149.
[33] N. Swamy, K.S. Persons, T.C. Chen, R. Ray, J. Cell. Biochem. 89 (2003) 909–916.
[34] N. Swamy, T.C. Chen, S. Peleg, P. Dhawan, S. Christakos, L.V. Stewart, N.L. Weigel, R.G. Mehta, M.F. Holick, R. Ray, Clin. Cancer Res. 10 (2004) 8018–8027.
[35] T.S. Lange, R.K. Singh, K.K. Kim, Y. Zou, S.S. Kalkunte, G.L. Sholler, N. Swamy, L. Brard, Chem. Biol. Drug Des. 70 (2007) 302–310.